

VIII. Solid Propellant Engineering

PROPULSION DIVISION

A. Surface Temperature Relationships for Ignition Material Deflagration Onset, O. K. Heiney

1. Introduction

For many electroexplosive applications it is necessary to know or be able to predict the temperature at which deflagration onset will occur in ignition mix materials. The element of the explosive train of interest here is the ignition bead chemicals immediately in contact with and ignited by a heated bridgewire. These materials are normally a heavy metal-oxidizer mixture bonded to the bridgewire with a nitrocellulose paste. The purpose of the experimental effort is to ignite materials whose thermal and chemical properties are carefully controlled with a bridgewire at varying known energy input rates. With proper analysis, the conventional power versus time-to-fire curve would then give an ignition temperature-time relationship, providing, hopefully, a constant temperature ignition criterion or a regular temperature-time-to-fire dependence.

2. Analysis and Procedure

The electroexplosive system used is as illustrated in Fig. 1. The ignition temperature is that at the mix wire interface at the time the ignition explosion destroys the wire.

Thermal energy input to the system is, of course, provided by large metered pulses of electrical current flow in the highly resistant wire. With the known electrical and thermal properties of nichrome and the ignition material, an interface temperature expression may be formulated from a solution provided for this type problem by Ref. 1, Sec. 13.8.

For a heat generation rate in region A of Q_0 , the quoted solution as a function of time is then

$$T - T_0 = \frac{4Q_0 K_2 k_2}{\pi^2 a} \int_0^\infty \frac{[1 - \exp(-k_1 u^2 t)] J_0(ur) J_1(ua) du}{u^4 [\phi^2(u) + \psi^2(u)]} \quad (1)$$

with u being a dummy variable of integration

$$K = (K_1/K_2)^{1/2}$$

and

$$\psi(u) = K_1 k_2^{1/2} J_1(au) J_0(Kau) - K_2 k_1^{1/2} J_0(au) J_1(Kau)$$

$$\phi(u) = K_1 k_2^{1/2} J_1(au) Y_0(Kau) - K_2 k_1^{1/2} J_0(au) Y_1(Kau)$$

J_0 and J_1 are zero and first-order Bessel functions of the first kind, and Y_0 and Y_1 are zero and first-order Bessel

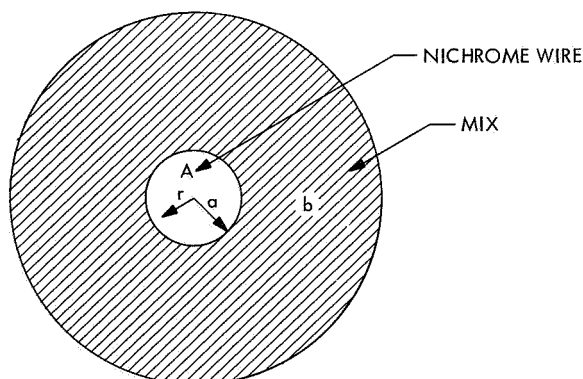


Fig. 1. Bridgewire ignition bead system

functions of the second kind, respectively. The remainder of the notation is as listed in Table 1.

To determine the temperature at the interface of the wire and mix for a given firing it is necessary to set $r = a$, input the appropriate values of Q_0 and t , and numerically integrate (by computer) Eq. (1) on the dummy variable.

Accomplishment of the above requires, however, detailed knowledge of the thermal properties of both nichrome wire and the ignition materials of interest. The data on the nichrome wire are available in the literature (Refs. 2 and 3). The data on the specific heat and heat conductivity for the ignition mixes had to be experimentally derived. The mixes were designated X-26 for a zirconium-ammonium perchlorate formulation and X-29 for a zirconium-barium chromate type.

Specific heats for both were determined at various temperatures on a differential scanning calorimeter by means of comparison with a synthetic sapphire (Al_2O_3) reference

Table 1. Definition of terms

a	= radius of wire
E_A	= lumped activation energy of ignition reaction
k_1	= thermal diffusivity of wire
k_2	= thermal diffusivity of ignition mix
K_1	= thermal conductivity of wire
K_2	= thermal conductivity of ignition mix
Q_0	= energy generation rate per unit volume in wire
r	= arbitrary radius reference
T_0	= ambient temperature
T	= wire mix interface temperature
u	= dummy variable of integration
τ	= specific time to fire

whose specific heat at various temperatures is precisely known. Results are as tabulated on Table 2.

Table 2. Specific heats of X-26 and X-29

Temperature, °C	Specific heat, cal/g/°C	
	X-26	X-29
50	0.142	0.129
100	0.150	0.137
150	0.161	0.149
175	0.170	0.154

The heat conductivity of the materials was determined by a guarded hot plate method very similar to that described in ASTM procedure C-177 (Ref. 4). These results are given on Table 3.

Table 3. Heat conductivities of X-26 and X-29

Temperature, °C	Heat conductivity, cal/s/cm ² /°C	
	X-26	X-29
50	7.2×10^{-4}	8.3×10^{-4}
100	7.4×10^{-4}	8.4×10^{-4}
150	7.6×10^{-4}	8.6×10^{-4}
175	7.9×10^{-4}	8.9×10^{-4}

These data with the densities of the materials (X-26: 1.84 g/cm³; X-29: 2.10 g/cm³) provide the necessary constants for the evaluation of Eq. (1) for each firing. The interface temperatures computed are described below.

3. Results

The experimental curves for power input versus time to fire are shown in Fig. 2 for X-26 and X-29. They are typical squib firing plots in that they can be divided into a linear or constant energy regime, transition region, and finally a constant power line. Using Eq. (1) and the techniques described in the analysis section, these data may be transformed into an ignition temperature versus time plot as shown in Fig. 3. These figures graphically illustrate the fact that at short ignition-time intervals it is incorrect to assume or prescribe a constant ignition temperature to a given ignition material. The temperatures at ignition range from 2200 to 250°C for X-26 and 1350 to 240°C for X-29, dependent upon rate of heat input. The lower range temperatures correlate quite well with crucible furnace ignition data which indicates mass cook-off temperatures of 215°C for X-26 and 225°C for X-29.

In light of the marked dependence of ignition temperature on time to fire, it is plausible to anticipate an

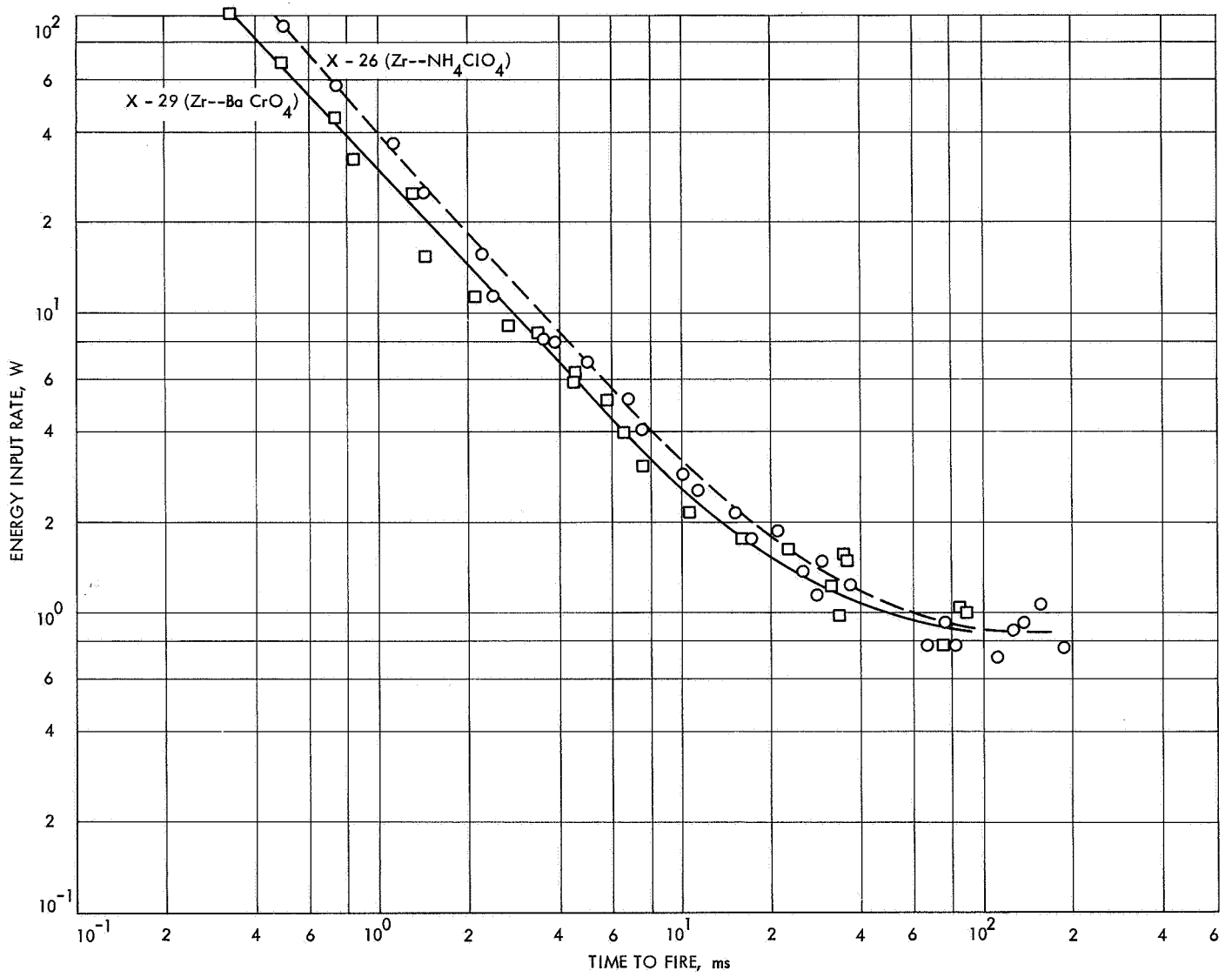


Fig. 2. Power versus time to fire Zr-NH₄ClO₄ (X-26) and Zr-BaCrO₄ (X-29)

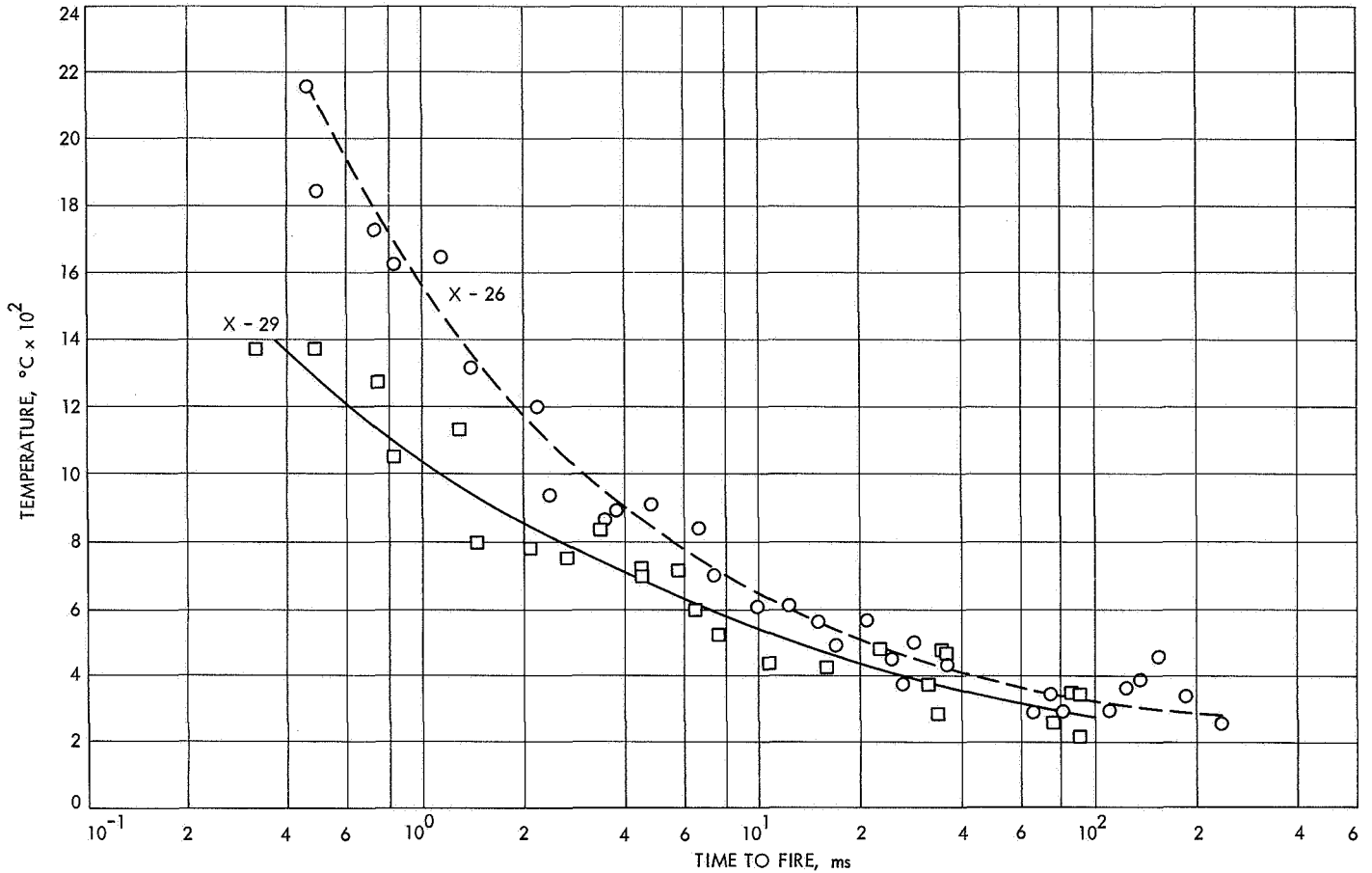


Fig. 3. Temperature at ignition versus time to fire $\text{Zr-NH}_4\text{ClO}_4$ (X-26) and Zr-BaCrO_4 (X-29)

Arrhenius-type time dependence for the ignition reaction; that is

$$\frac{dc}{dt} = r = Ae^{-\frac{E_a}{RT}}$$

$$r = 1/\tau$$

Then it follows that

$$\ln \tau \sim \frac{1}{T}$$

With the exception of the monotonically increasing time-variant temperature, this argument is similar to that used to predict thermal explosion times for various reactive gas mixtures.

Figure 4 shows plots of $\ln \tau$ versus the reciprocal temperature, each of which would be expected to display a straight line if the above argument were valid. It is seen that the points tend to be somewhat skewed, and no such simple relationship is identifiable.

4. Conclusions

The conclusions of this analytic and experimental effort are largely negative. No single ignition temperature was found; neither was there an explicit, simple, fundamental relationship between ignition temperature and time to fire. It should be realized that the conductivity and diffusivities are functions of temperature, and that the form of Eq. (1) requires that mean values be used. The effects in the numerator and denominator tend to stabilize the results, but the absolute temperature values of the very short firing time cases are inherently less accurate than the lower temperature cases. This fact does not, however, affect the soundness of the basic conclusion; which is that the prescribing of a single ignition temperature for short thermal induction times is neither accurate nor reasonable.

References

1. Carslaw, H. S., and Jaeger, J. C., *Conduction of Heat in Solids*, Oxford University Press, 1959.

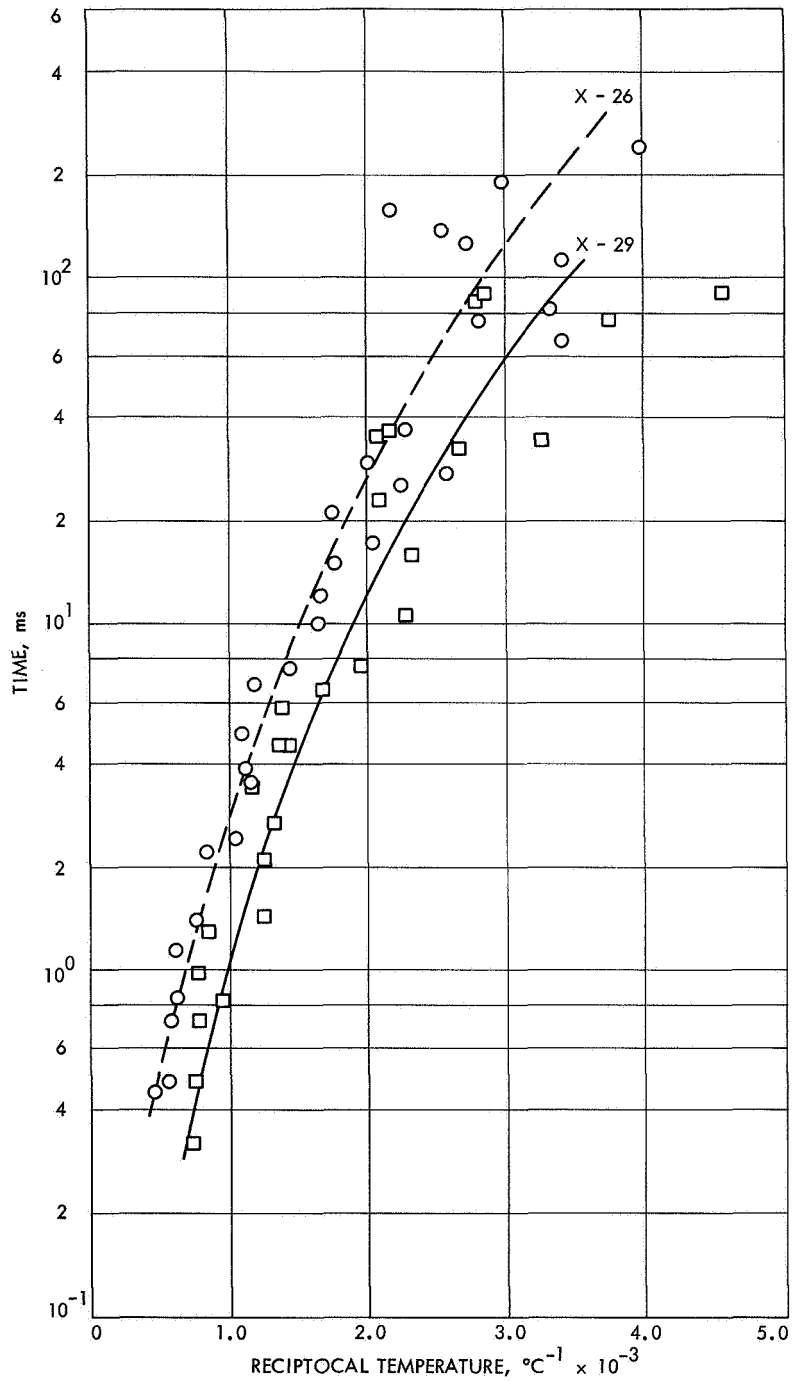


Fig. 4. Time to fire versus reciprocal of ignition temperature

2. Silverman, L., "Thermal Conductivity Data," J. Metals, Vol. 5, pp. 631-632, 1953.
3. Douglas, T. B., and Dever, J. L., J. Res. NBS, Vol. 54, No. 1, pp. 15-19, 1955.
4. *Thermal Conductivity of Materials by Means of the Guarded Hot Plate*, American Society of Testing Materials, ASTM Standard C177, 1963.

B. Applications Technology Satellite Motor Development, R. G. Anderson and R. A. Grippi

1. Introduction

Previous reports of progress on the development of the ATS motor have been published in SPS 37-20 to 37-33, Vol. V, SPS 37-34 to 37-45, Vol. IV, and SPS 37-47 to 37-49, Vol. III. As of this date the formal motor development and qualification phases are complete.

2. Program Status

Three flight units, processed in September 1966, were used to support the successfully launched ATS-B (December 1966) and ATS-C (November 1967) satellites. The spare flight unit (code Z-1) has been returned to JPL-Edwards Test Station (JPL-ETS) and placed into ambient storage. This spare unit will remain at ambient temperature conditions until September 1969, at which time it will be inspected, X-rayed, and static-fired. The testing of unit Z-1, 3 yr after it was cast, will extend the storage characteristics of the ATS apogee unit by 1 yr. The original storage program (SPS 37-48, Vol. III) verified motor integrity for a period of 2 yr by the testing of three units, one each after 16, 20, and 24-mo aging periods.

During March and April 1968, the last four ATS apogee flight units were cast. Unit Z-7 was processed to flight standards and static-tested at the JPL-ETS as a confirmation unit for the three remaining flight units (Z-4, Z-5 and Z-6). The fourth ATS satellite (ATS-D) was unsuccessfully launched on August 10, 1968. The remaining ATS satellite (ATS-E) is presently scheduled for an April-May 1969 launch.

3. Static Test of Motor Z-7

Apogee unit Z-7 was static-tested on May 9, 1968. This unit was flight quality and was processed to established flight-loading procedures. Prior to static testing, the unit was subjected to a temperature cycle of 10, 110, and 10°F and returned to ambient temperature for visual and

radiographic inspection. The unit was static-fired with a grain temperature of 10°F while spinning at 150 rev/min. Postfire inspection of the motor hardware indicated normal performance and operation during its 43-s run. Table 4 lists the static test summary for this unit.

Table 4. ATS Apogee motor flight test motor Z-7 static test summary

Test conditions	
Type	Atmospheric-spin
Location	JPL-ETS
Date	May 9, 1968
Run No.	E-884
Grain temperature, °F	10
Propellant weight, lb	760.5
Pressure data	
Characteristic velocity, W^* , ft/s	4959
Chamber pressure integral, psia-s	8905
Igniter peak pressure, psia (ms)	2032 (18)
Chamber ignition peak pressure, psia (ms)	259 (28)
Chamber starting pressure, psia (s)	103 (0.18)
Chamber run peak pressure, psia (s)	251 (33.5)
Time	
Ignition delay, ms	6
Run time, s	43.44
Nozzle dimensions	
Throat diameter, in.	
initial	4.085
final	4.106
average	4.096
Throat erosion area, %	1.03

4. ATS-D Launch

Two apogee flight units (Z-4 and Z-5) were shipped by ground transportation to the Air Force Eastern Test Range (AFETR) for support of the ATS-D launch.

After three weeks of flight preparation, the units received visual inspection, propellant grain X-ray, and motor assembly pressure testing. After these initial inspections unit Z-4 was returned to storage, and unit Z-5 was completed for flight use. Flight completion includes the mating of the igniter to the safe-and-arm device, the installation and orientation of the igniter to apogee motor, the installation of the apogee unit to the spacecraft, and the installation of the apogee motor's thermal blankets. When the apogee unit is secured to the spacecraft, JPL's

flight support functions are essentially complete. Table 5 lists the weight data for the Z-4 and Z-5 apogee units.

The ATS-D was launched on August 10, 1968. A malfunction in the *Centaur* engine prevented a second engine burn, leaving the spacecraft/apogee motor/*Centaur* in a 100- by 400-nm parking orbit. The Goddard Space Flight Center indicates that the orbiting package will reenter the earth's atmosphere approximately 2 mo after launch.

The ATS-D and the ATS-E (final satellite in the ATS program) are both synchronous-altitude gravity-gradient-stabilized satellites. The ATS-E is tentatively scheduled for April-May of next year. JPL has two apogee units to support this final launch. The Z-4 apogee unit is presently in storage at AFETR. The Z-6 apogee unit has been cast and is in storage at JPL-ETS. This unit will be inspected, assembled, and shipped to AFETR during the first quarter of 1969.

Table 5. Weight data for ATS-D apogee units

Part	Weight, lb	
	Unit Z-4 ^a Chamber T-19 Nozzle F-33	Unit Z-5 ^b Chamber T-21 Nozzle F-48
Chamber ^c	36.69	37.36
Nozzle ^d	38.10	37.15
Miscellaneous ^e	0.37	0.37
Igniter	1.00	1.00
Safe and arm	5.00	5.00
Total inerts	81.16	80.88
Propellant	759.50	760.00
Total motor weight	840.66	840.88
^a Flight preference: backup for ATS-D and E. ^b Flight preference: prime for ATS-D. ^c Chamber includes chamber insulation, curing agent, and lead balance weight. ^d Nozzle includes diaphragm and balance weight. ^e Miscellaneous includes 36 screws and washers, O-ring, and nozzle lock wire.		